Transport of Spin Magnetic Multipole Moments Carried by Bloch Quasiparticles

Muhammad Tahir and Hua Chen

Phys. Rev. Lett. **131**, 106701 — Published 6 September 2023

DOI: 10.1103/PhysRevLett.131.106701

Transport of Spin Magnetic Multipole Moments Carried by Bloch Quasiparticles

Muhammad Tahir[1] and Hua Chen[1,2]

[1] *Department of Physics, Colorado State University, Fort Collins, CO 80523, USA*
[2] *School of Advanced Materials Discovery, Colorado State University, Fort Collins, CO 80523, USA*

Magnetic ordering beyond the standard dipolar order has attracted significant attention in recent years, but it remains an open question how to effectively manipulate such nontrivial order parameters using external perturbations such as electric currents or fields. In particular, it is desirable to have a conceptual tool similar to nonequilibrium spin currents in spintronics to describe the creation and transport of multipole moments. In this context, we present a theory for Cartesian spin magnetic multipole moments of Bloch quasiparticles and their transport based on a general gauge-invariant formula obtained using the wave packet approach. As a concrete example, we point out that the low-energy Hamiltonian of phosphorene subject to a perpendicular electric field has a valley structure that hosts magnetic octupole moments. The magnetic octupole moments can be exhibited by an in-plane electric current and lead to accumulation of staggered spin densities at the corners of a rectangular sample. Our work paves the way for systematically seeking and utilizing quasiparticles with higher-order magnetic multipole moments in crystal materials towards the emergence of multipole-tronics.

Introduction.—Antiferromagnets, whose order parameters can be generally described by higher-order electromagnetic multipole moments [1–5], have recently received significant interest in several condensed matter communities [6–31]. For certain collinear or noncollinear antiferromagnets whose magnetic order transforms similarly as the magnetic dipole, it has been established in recent years that they can be measured using experimental setups designed for phenomena in ferromagnets, e.g. the anomalous Hall effect, anomalous Nernst effect, magneto-optical Kerr effect, etc., and be manipulated using uniform magnetic fields coupled through the symmetry-allowed weak net magnetization [32–47]. However, it is imperative now to go beyond this paradigm to fully exploit the potential of antiferromagnets from the perspective of their unique multipolar degrees of freedom, especially considering the establishment of new experimental techniques that can potentially access non-dipolar magnetic order parameters directly, such as nitrogen-vacancy imaging [48–50], nonlinear transport [51], etc.

On the other hand, the rapid development of spintronics in the past decades has suggested that quasiparticle currents carrying the appropriate quantum number–spin, even if it is not exactly conserved, can be highly useful both as a conceptual tool and as a practical means for designing experiments and devices [52–59]. This is because arguments based on the spin current language still have the correct symmetry that allows the corresponding effects to occur [60, 61]. It is therefore meaningful to discuss transport of non-conserved quantities [62, 63] with the purpose of motivating experimental and theoretical searches of new measurable effects. However, an immediate difficulty arises when one tries to generalize quasiparticle spin currents to that of multipole moments. That is, multipole moments being local (both in real and momentum spaces) objects are not as well defined as spin for Bloch electrons due to the appearance of position operator in their definition.

For several low-order electric and magnetic multipole moments of extended equilibrium systems, theories have been developed in recent years to address the apparent origin and gauge dependences [17–20, 64–70]. In particular, for multipole moments that do not have an inherent gauge dependence (such as electric polarization), a thermodynamic approach can be used to obtain their gauge-invariant forms [17–20, 68, 70]. Such a procedure can also be applied to higher-order spin magnetic multipole moments [71]. However, since it only gives the multipole moments of an extended system in equilibrium, the thermodynamic approach does not address the issue of defining local objects for individual quasiparticles.

Having well-defined multipole moments attached to individual quasiparticles is useful in developing semiclassical pictures of nonequilibrium multipole phenomena that involve boundaries or interfaces. This is in parallel to fully quantum mechanical response theories that rely on physical observables directly determined experimentally (e.g. local spin densities rather than spin currents in spin-Hall-related phenomena [60, 61, 72–75]) and has its own advantages. For example, in the context of valleytronics [76], one can look for new materials that host well-defined multipole moments at different valleys, similar to the orbital magnetic moments in monolayer 2H transition-metal dichalcogenides [77–79], so that a selective creation of quasiparticles in such valleys and their currents directly leads to the corresponding multipolar observables.

In this Letter we provide a framework for obtaining arbitrary-order Cartesian spin magnetic multipole moments of Bloch quasiparticles, which is analogous to the wave-packet understanding of spin magnetic dipole moment of Dirac electrons [80, 81]. Based on it we introduce a semiclassical Boltzmann theory for the transport of spin magnetic multipole moments and apply it to a prototypi-

cal example of monolayer phosphorene. As schematically illustrated in Fig. 1, Bloch wave packets carrying spin magnetic octupole moment $\mathcal{M}^x_{xy}$ (defined below) can be excited by an in-plane electric current, which further lead to accumulation of spins with staggered signs at the four corners of a rectangular sample.

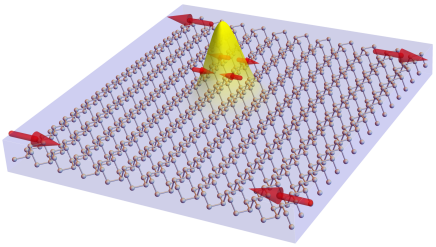

FIG. 1. Schematic illustration of a wave packet carrying $\mathcal{M}^x_{xy}$ and the corresponding corner spin pattern in a macroscopic monolayer phosphorene sample with Rashba spin-orbit coupling.

Spin magnetic multipole moments of Bloch wave packets.—2^l-th order Cartesian spin magnetic multipole moments of a continuous spatial distribution of spin density are defined classically through Taylor expansion of the Zeeman energy as

$$\mathcal{M}^{i_l}_{i_1,i_2,\ldots,i_{l-1}} \equiv -\frac{g\mu_B}{\hbar}\int d^3\mathbf{r} s^{i_l}(\mathbf{r}) r_{i_1} r_{i_2}\ldots r_{i_{l-1}} \quad (1)$$

where $g\approx 2$ is the Landé g-factor, μ_B is the Bohr magneton, and $i_{1,2,\ldots l}$ label Cartesian axes. For simplicity in this work we ignore the overall factor $-g\mu_B/\hbar$. Promoting the spin density to an expectation value of the spin density operator $\hat{\mathbf{s}}\delta(\hat{\mathbf{r}}-\mathbf{r})$ then converts Eq. (1) to an expectation value of the multipole moment operator

$$\hat{\mathcal{M}}^{i_l}_{i_1,i_2,\ldots,i_{l-1}} \equiv \hat{s}^{i_l}\hat{r}_{i_1}\hat{r}_{i_2}\ldots\hat{r}_{i_{l-1}}. \quad (2)$$

Our first task is to examine its expectation value in a Bloch wave packet state. A wave packet of a non-degenerate Bloch band labeled by n at momentum $\mathbf{k}_c$ is defined as $|W\rangle = \int_{\mathrm{BZ}} d^3\mathbf{k} w_{\mathbf{k}}|n\mathbf{k}\rangle$ where $w_{\mathbf{k}}$ is a scalar function localized at $\mathbf{k}=\mathbf{k}_c$. The case of degenerate bands which requires the consideration of non-Abelian gauge transformation [82, 83] will be discussed in a future work, but our approach applies to the situation that such degeneracies can be lifted by infinitesimal external perturbations.

The naive expectation value

$$(\mathcal{M}^g)^{i_l}_{i_1 i_2\ldots i_{l-1}} \equiv \langle W|\hat{\mathcal{M}}^{i_l}_{i_1,i_2,\ldots,i_{l-1}}|W\rangle \quad (3)$$

is, however, clearly dependent on the choice of origin, which is expected since it is the case for classical multipole moments Eq. (1) as well [84]. Nonetheless, the localized nature of a wave packet makes it sensible to define multipole moments by using the center-of-mass position $\mathbf{r}_c$ as the origin [17, 18, 66–68, 80, 81]. For the low-order ($l\le 3$) multipole moments considered in these literature the resulting formulas are also gauge-invariant, making it meaningful to discuss the transport of such observables by the center-of-mass motion of the wave packets. However, at higher orders ($l>3$) simply replacing $\mathbf{r}$ by $\mathbf{r}-\mathbf{r}_c$ does not in general lead to a gauge-invariant expression, nor is the result independent of the wave packet shape [85].

Instead, we introduce the following formula for a general 2^l spin magnetic multipole moment of a Bloch quasiparticle:

$$\mathcal{M}^{j_l}_{j_1 j_2\ldots j_{l-1}} \equiv \quad (4)$$
$$\mathcal{N}^{-1}\mathrm{Re}\sum_{\{j\}^{\mathrm{u}}_{l-1}}\langle u_{n\mathbf{k}}|s_{j_l}\prod_{j\in\{j\}^{\mathrm{u}}_{l-1}}(i\partial_{k_j}-\mathcal{A}_j)|u_{n\mathbf{k}}\rangle\big|_{\mathbf{k}=\mathbf{k}_c}$$

where $|u_{n\mathbf{k}}\rangle$ is the periodic part of the Bloch state $|n\mathbf{k}\rangle$; the Berry connection $\mathcal{A}_j \equiv \langle u_{n\mathbf{k}}|i\partial_{k_j}|u_{n\mathbf{k}}\rangle$; the summation is over all unique permutations of $l-1$ elements $\{j_1,\ldots,j_{l-1}\}$, denoted by $\{j\}^{\mathrm{u}}_{l-1}$. The normalization factor $\mathcal{N}=(l-1)!/(N_x!N_y!N_z!)$ where N_j is the number of times that the Cartesian index j appears in the set $\{j_1,\ldots,j_{l-1}\}$.

Eq. (4) is both gauge-invariant and independent of the wave-packet shape $w_{\mathbf{k}}$. Details of its derivation are relegated to Sec. I of [85]. The central idea is to use the following identity:

$$(i\partial_x - A - i\partial_x\ln|g| + \partial_x\arg g)^n(gf) = g(i\partial_x - A)^n f \quad (5)$$

where $n>0$ is an arbitrary integer, A, g, f are arbitrary functions of the variable x, with g additionally required to have nonvanishing norm and smooth argument across potential branch cuts. Eq. (5) allows one to eliminate terms resulting from smooth transformations of $|W\rangle$ that maintain the center-of-mass crystal momentum $\mathbf{k}_c$. Alternatively, one can obtain Eq. (4) from a heuristic approach [85] by replacing $\hat{\mathbf{r}}$ by $\hat{\mathbf{r}}-\hat{\mathbf{r}}_c$ in Eq. (3) with $\hat{\mathbf{r}}_c$ the re-quantized center-of-mass position [81, 87].

Eq. (4) reproduces the wave-packet contributions in the previous results of spin quadrupole or toroidal moments [85]. As new formulas resulting from Eq. (4) we give below those for the spin octupole ($l=3$) and hexadecapole ($l=4$) [30] moments:

$$\mathcal{M}^c_{ab} = -\langle s_c\partial_a\partial_b\rangle\big|_{\boldsymbol{\mathcal{A}}=0} \quad (6)$$
$$\mathcal{M}^d_{abc} = -\frac{1}{6}\langle is_d\partial_a\partial_b\partial_c\rangle\big|_{\boldsymbol{\mathcal{A}}=0} + \frac{1}{6}\partial_a\partial_b\mathcal{A}_c\langle s_d\rangle\big|_{\boldsymbol{\mathcal{A}}=0}$$
$$+\frac{1}{6}[\partial_a\mathcal{A}_b\langle s_d\partial_c\rangle + \partial_b\mathcal{A}_c\langle s_d\partial_a\rangle + \partial_a\mathcal{A}_c\langle s_d\partial_b\rangle]\big|_{\boldsymbol{\mathcal{A}}=0}$$
$$+(a,b,c\,\text{permutations})$$

where $\langle\ldots\rangle \equiv \mathrm{Re}\langle u_{n\mathbf{k}}|\ldots|u_{n\mathbf{k}}\rangle$. Note that $\boldsymbol{\mathcal{A}}=0$ does not necessarily mean that the derivatives of $\boldsymbol{\mathcal{A}}$ also vanish. Eq. (6) can be used together with the explicit formulas of the $\mathbf{k}-$derivatives of $|u_{n\mathbf{k}}\rangle$ given in Sec. II of [85] in model or first-principles calculations.

Semiclassical transport of spin magnetic multipole moments and its physical consequences.—Since the spin magnetic multipole moments Eq. (4) are properties of individual Bloch quasiparticles $|n\mathbf{k}\rangle$, their creation in real space by external perturbations can be formulated as quasiparticle excitations, i.e. intra-band contributions to the nonequilibrium density matrix, induced by the perturbations. The intra-band contributions are also expected to be dominant in clean systems with a long relaxation time.

Such intra-band contributions can be conveniently obtained from semiclassical Boltzmann theory. For example, up to first order in the electric field $\mathbf{E}$, the Boltzmann equation with a constant relaxation time τ gives the nonequilibrium distribution function $f^{(1)} = e\tau\frac{\partial f_0}{\partial\epsilon_{n\mathbf{k}}}\mathbf{v}_{n\mathbf{k}}\cdot\mathbf{E}$, which leads to the nonequilibrium spin magnetic multipole moment density

$$\langle\mathcal{M}\rangle = e\tau\sum_n\int\frac{d^D\mathbf{k}}{(2\pi)^D}\mathcal{M}_{n\mathbf{k}}\frac{\partial f_0}{\partial\epsilon_{n\mathbf{k}}}\mathbf{v}_{n\mathbf{k}}\cdot\mathbf{E} \tag{7}$$

where $\mathcal{M}_{n\mathbf{k}}$ is given by Eq. (4) and D stands for the spatial dimension of the system. One can similarly define a nonequilibrium multipole current density as

$$\langle\mathcal{M}\otimes\mathbf{v}\rangle = \sum_n\int\frac{d^D\mathbf{k}}{(2\pi)^D}\mathcal{M}_{n\mathbf{k}}\mathbf{v}_{n\mathbf{k}}g_{n\mathbf{k}} \tag{8}$$

where g is a general solution of the Boltzmann equation that can include higher-order terms in $\mathbf{E}$. Note that one can also use the Berry-curvature-corrected semiclassical Boltzmann theory to account for any anomalous transport coefficients [87, 97, 98], e.g., a Hall effect for the multipole current.

The above nonequilibrium quantities have corresponding macroscopic observables that can be intuitively understood using coarse-grained macroscopic Maxwell equations [84]. For example, uniform $\langle\mathcal{M}\rangle$ of different order corresponds to different boundary spin density distributions, with one example illustrated in Fig. 1 and discussed in detail below. $\partial\langle\mathcal{M}\rangle/\partial\mathbf{E}$ in Eq. (7) is a crossed susceptibility that can be measured if one can prepare quasi-static magnetic fields of nearly constant spatial gradients of the corresponding order. It is also possible to measure the magnetic multipole moment through the characteristic angular distribution of the multipole fields generated by a macroscopic sample.

In contrast, the nonequilibrium multipole current has similar issues as the spin current [62, 63, 99–102] since multipole moment is not a conserved quantity and the currents are not directly measured experimentally. It is therefore better used as a conceptual tool for understanding nonlocal transport phenomena. For example, one can use symmetry analysis to know if a Hall component of $\langle\mathcal{M}\otimes\mathbf{v}\rangle$ can be created by a given electric field in a nonmagnetic material, which can flow into a neighboring layer of another material with multipolar order and lead to dynamical responses of the order parameter.

Spin octupole moments in phosphorene.—In this section we give an example of the spin octupole moments in phosphorene subject to a perpendicular electric field. Monolayer phosphorene has a puckered honeycomb structure formed by P atoms as depicted in Fig. 2 (a). The buckling reduces 3-fold symmetries in the honeycomb lattice to 2-fold D_{2h} symmetry and suggests its potential for Cartesian spin octupole moments. The low-energy Hamiltonian of multi-layer black phosphorous has been shown to be [90–93, 103–105] $h_0(\mathbf{k}) = \left(\frac{\hbar^2k_y^2}{2m_y}+\Delta\right)\sigma_x - \hbar v_x k_x\sigma_y$ where $\boldsymbol{\sigma}$ and $\mathbf{s}$ are the Pauli matrix vectors in the pseudospin and real spin basis, respectively, and Δ is a gap of structural origin.

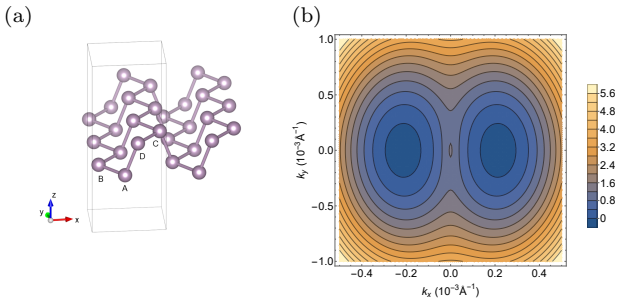

FIG. 2. (a) Structure of monolayer phosphorene. (b) Contour plot of the eigenenergy (in units of μeV) for the lower conduction band of monolayer phosphorene minus Δ.

All bands are doubly degenerate in pristine phosphorene due to spatial inversion symmetry. We therefore consider a Rashba-type spin-orbit coupling induced by a perpendicular electric field. The Rashba term in the continuum model is found to be [85]

$$h_R(\mathbf{k}) = \Lambda_0^R\sigma_y s_y + \Lambda_1^R k_y\sigma_x s_x - \Lambda_2^R k_x\sigma_x s_y \tag{9}$$

where $\Lambda_{0,1,2}^R$ are constants depending on the lattice parameters as well as the Rashba spin-dependent hopping in the tight-binding model. h_R is consistent with previous DFT results [94, 106]. Ignoring the less important Λ_2^R [85] allows us to diagonalize $h = h_0 + h_R$ analytically and to find two extrema of the bands at $\pm\mathbf{K}_v = \pm\Lambda_0^R/(\hbar v_x)\hat{x} \approx \pm 2\times10^{-4}\text{Å}^{-1}$ (estimated based on the DFT results for a 2.6 V/Å electric field in [94]). This is consistent with Fig. 2 which shows a contour plot of the lower conduction band with Λ_2^R included.

We next focus on the center of each valley and consider the octupole component $\mathcal{M}_{xy}^k$ since such a component corresponds to a nontrivial staggered spin accumulation pattern at the corners of a rectangular sample. Eq. (6)

leads to [85]

$$\mathcal{M}^c_{ab} = \mathrm{Re}\sum_{m\neq n}\frac{(s_c)_{nn}(\partial_a H_{\mathbf{k}})_{nm}(\partial_b H_{\mathbf{k}})_{mn}}{(\epsilon_{n\mathbf{k}}-\epsilon_{m\mathbf{k}})^2} \quad (10)$$
$$-\mathrm{Re}\sum_{m\neq n}\frac{(s_c)_{nm}(\partial_a\partial_b H_{\mathbf{k}})_{mn}}{\epsilon_{n\mathbf{k}}-\epsilon_{m\mathbf{k}}}$$
$$-\mathrm{Re}\sum_{l\neq n,m\neq n}\left\{\frac{(s_c)_{nm}(\partial_b H_{\mathbf{k}})_{ln}(\partial_a H_{\mathbf{k}})_{ml}}{(\epsilon_{n\mathbf{k}}-\epsilon_{l\mathbf{k}})(\epsilon_{n\mathbf{k}}-\epsilon_{m\mathbf{k}})}+(a\leftrightarrow b)\right\}$$
$$+\mathrm{Re}\sum_{m\neq n}\left\{\frac{(s_c)_{nm}(\partial_b H_{\mathbf{k}})_{mn}(\partial_a H_{\mathbf{k}})_{nn}}{(\epsilon_{n\mathbf{k}}-\epsilon_{m\mathbf{k}})^2}+(a\leftrightarrow b)\right\}$$

Still ignoring Λ_2^R and considering the lower conduction band only, we found [85] that at the valley centers only $\mathcal{M}^x_{xy}\neq 0$, which in the limit of $\Lambda_0^R \ll \Delta$ becomes:

$$\mathcal{M}^x_{xy}(\mathbf{K}_v) \approx -\frac{\hbar^2 v_x \Lambda_1^R \Delta}{4(\Lambda_0^R)^3} \approx -1.66\times 10^6\,\text{Å}^2\cdot\frac{\hbar}{2} \quad (11)$$

Such a large result originates from the tiny splitting between the two conduction bands at the valley center, $\delta\epsilon(\mathbf{K}_v) \approx 2(\Lambda_0^R)^2/\Delta$. In practice this splitting must be greater than $\hbar/\tau_{\mathrm{qp}}$, where τ_{qp} is the finite lifetime of Bloch quasiparticles, for Eq. (11) to be relevant. Figure. 3 (a) plots $\mathcal{M}^x_{xy}$ for the lowest conduction band near the Brillouin zone center with Λ_2^R included, which gives $\mathcal{M}^x_{xy}(\mathbf{K}_v) = -1.54\times 10^6\,\text{Å}^2\cdot\frac{\hbar}{2}$, in good agreement with Eq. (11).

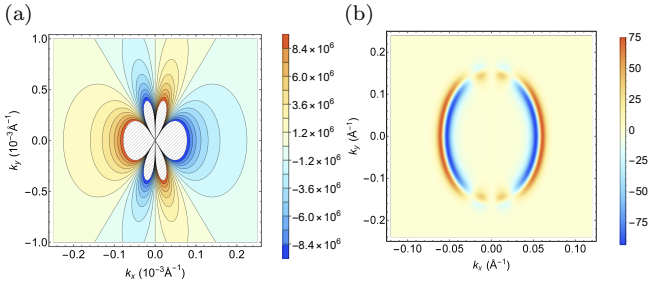

FIG. 3. (a) $\mathcal{M}^x_{xy}$ of the lowest conduction band of phosphorene in units of $\text{Å}^2\cdot\frac{\hbar}{2}$. The regions where its values become too large due to the vanishing spin-orbit splitting between the two conduction bands are crossed out for better illustration. (b) Integrand of Eq. (7) for $\mathcal{M}^x_{xy}$ with $E_F-\Delta = 0.1$ eV, $k_BT = 0.01$ eV, and $\mathbf{E}\parallel\hat{x}$.

We next discuss creation of the spin magnetic octupole moment in phosphorene driven by electric fields based on the semiclassical Boltzmann theory presented above. The integrand of Eq. (7) for $\mathcal{M}^x_{xy}$ with $E_F-\Delta = 0.1$ eV, $k_BT = 0.01$ eV, and $\mathbf{E}\parallel\hat{x}$ is shown in Fig. 3 (b). The contribution due to each conduction band can be seen to have a nonzero Fermi surface integral, although the two bands have opposite contributions which largely cancel each other. Taking $\hbar/\tau = 0.1$ eV, the result of Eq. (7) per electric field in the units of V/Å is $-1.65\times 10^{-2}\,\frac{\hbar}{2}$ (assuming the same 2.6 V/Å perpendicular field).

To understand the implication of this result, we note that a rectangular sample with a uniform $\mathcal{M}^x_{xy}$ density has an approximate spatial dependence $\mathcal{M}^x_{xy}(\mathbf{r}) \approx \mathcal{M}^x_{xy}\Theta[\pm(x-x_c)]\Theta[\pm(y-x_c)]$ near a given corner bounded by $x = x_c$ and $y = y_c$, where $\Theta(x)$ is the step function. The local spin at a given corner is therefore obtained as [84] $S^x_c = \int_c d^2\mathbf{r}\partial_x\partial_y\mathcal{M}^x_{xy}(\mathbf{r}) = \pm\mathcal{M}^x_{xy}$, where the integration is in a small region near the corner where the integrand is significant. The positive (negative) sign is taken when the arguments of the two step functions have the same sign (opposite signs), resulting in the corner spin pattern in Fig. 1.

With this understanding, the above current-induced octupole moment in phosphorene is equivalently described as a corner-spin-electric-field response with the rough size of $-1.65\times 10^{-2}\,\frac{\hbar}{2}\text{V}^{-1}\text{Å}$. For comparison one can calculate the current-induced uniform spin density due to the Rashba spin-orbit coupling. The same set of parameters give a y-spin density of $-4.8\times 10^{-4}\,\mu_B/\text{Å}^2$ per 1 V/Å electric field along x. However, the octupole-induced corner spin is orthogonal to the uniform spin density and should therefore be able to be isolated using magnetic imaging techniques that are sensitive to local spin orientations, such as Lorentz TEM. In [85] we further showed that the boundary spin density due to current-induced quadrupole moment is also orthogonal to that due to the octupole moment and can therefore be separated out.

Finally, we point out that a current along x and carrying the octupole moment $\mathcal{M}^x_{xy}$ can be created by a nonlinear response to E_x. Such a current does not arise from linear response since it is forbidden by symmetry [85], which can also be seen from Fig. 3 (b). In general, if a multipole moment vanishing in equilibrium becomes nonzero through linear response to an electric field, a second-order response to the same electric field can drive a current of that multipole moment.

Discussion.—Our work only discussed semiclassical transport based on the intrinsic multipole moments of Bloch quasiparticles. Equilibrium and nonequilibrium macroscopic multipole moments of a finite system in general involve more contributions due to boundary and inter-band terms [71, 107]. The former, similar to the situation of spin-orbit torques, depends on the boundary condition and is entangled with the bulk contribution due to spin non-conservation. Complementary insights may be obtained by the thermodynamic approach (for the equilibrium case) and by explicitly calculating the spin density responses at the boundary (for the nonequilibrium case) [60, 61]. The latter, for well-defined susceptibilities (i.e., not involving multipole currents), can be captured by linear or nonlinear response theories and will be left for a future work.

Our work shows that gauge dependence and origin dependence can be separate issues in studying multipole moments of quantum condensed matter systems. On the

one hand, classical multipole moments in general depend on origin. On the other hand, explicitly fixing the origin does not necessarily fix the gauge for a quantum multipole moment, since the former only sets a linear-in-$\mathbf{k}$ phase of the gauge transformation.

Separately, higher-order semiclassical theories based on the wave-packet approach in general include quantities that depend on the wave packet shape [108, 109]. Such shape dependence must be compensated by other contributions to the final macroscopic observable for a given system, although it can also be potentially exposed by experiments on individually prepared wave packets. In this regard, we expect the shape-independent wave-packet spin multipole moment given in this work to be most suitable for describing diffusive transport among spatially separated subsystems.

Our gauge-invariant formula can also be applied to electric multipole moments of Bloch wave packets. In particular, we note that "composite" contributions to the wave packet spin multipole moments can arise as products of lower-order spin and electric (without the factor of e) multipole moments of the wave packet. Such terms are not considered here but will turn out to be relevant when comparing the wave packet and thermodynamic approaches to the equilibrium multipole moments [71].

For prototypical materials hosting magnetic multipole moments in nonequilibrium, besides phosphorene, multilayer black phosphorus should also work since it has a similar low-energy Hamiltonian [91]. In three dimensions it will be interesting to look for hexadecapole moments with xyz spatial indices, since they lead to staggered corner spins in a cubic sample. We expect orthorhombic materials with either time-reversal or inversion symmetry broken to be promising candidates for observing them.

MT and HC were supported by NSF CAREER grant DMR-1945023. The authors are grateful to Qian Niu and Yang Gao for valuable discussions.

[1] A. F. Andreev, Magnetic properties of disordered media, Soviet Physics Uspekhi **21**, 541 (1978).
[2] A. F. Andreev and V. I. Marchenko, Symmetry and the macroscopic dynamics of magnetic materials, Soviet Physics Uspekhi **23**, 21 (1980).
[3] I. Dzyaloshinskii, External magnetic fields of antiferromagnets, Solid State Communications **82**, 579 (1992).
[4] A. F. Andreev, Macroscopic magnetic fields of antiferromagnets, Journal of Experimental and Theoretical Physics Letters **63**, 758 (1996).
[5] D. N. Astrov, N. B. Ermakov, A. S. Borovik-Romanov, E. G. Kolevatov, and V. I. Nizhankovskii, External quadrupole magnetic field of antiferromagnetic Cr2O3, Journal of Experimental and Theoretical Physics Letters **63**, 745 (1996).
[6] Y. Kuramoto, H. Kusunose, and A. Kiss, Multipole Orders and Fluctuations in Strongly Correlated Electron Systems, Journal of the Physical Society of Japan **78**, 072001 (2009), https://doi.org/10.1143/JPSJ.78.072001.
[7] P. Santini, S. Carretta, G. Amoretti, R. Caciuffo, N. Magnani, and G. H. Lander, Multipolar interactions in f-electron systems: The paradigm of actinide dioxides, Rev. Mod. Phys. **81**, 807 (2009).
[8] A. Sakai and S. Nakatsuji, Kondo Effects and Multipolar Order in the Cubic PrTr2Al20 (Tr=Ti, V), Journal of the Physical Society of Japan **80**, 063701 (2011), https://doi.org/10.1143/JPSJ.80.063701.
[9] T. Onimaru, K. T. Matsumoto, Y. F. Inoue, K. Umeo, T. Sakakibara, Y. Karaki, M. Kubota, and T. Takabatake, Antiferroquadrupolar Ordering in a Pr-Based Superconductor $PrIr_2Zn_{20}$, Phys. Rev. Lett. **106**, 177001 (2011).
[10] T. Onimaru and H. Kusunose, Exotic Quadrupolar Phenomena in Non-Kramers Doublet Systems — The Cases of PrT2Zn20 (T = Ir, Rh) and PrT2Al20 (T = V, Ti) —, Journal of the Physical Society of Japan **85**, 082002 (2016), https://doi.org/10.7566/JPSJ.85.082002.
[11] K. Kubo and Y. Kuramoto, Octupole Ordering Model for the Phase IV of CexLa1-xB6, Journal of the Physical Society of Japan **73**, 216 (2004), https://doi.org/10.1143/JPSJ.73.216.
[12] D. Mannix, Y. Tanaka, D. Carbone, N. Bernhoeft, and S. Kunii, Order Parameter Segregation in $Ce_{0.7}La_{0.3}B_6$: $4f$ Octopole and $5d$ Dipole Magnetic Order, Phys. Rev. Lett. **95**, 117206 (2005).
[13] K. Kuwahara, K. Iwasa, M. Kohgi, N. Aso, M. Sera, and F. Iga, Detection of Neutron Scattering from Phase IV of Ce0.7La0.3B6: A Confirmation of the Octupole Order, Journal of the Physical Society of Japan **76**, 093702 (2007), https://doi.org/10.1143/JPSJ.76.093702.
[14] T. Matsumura, T. Yonemura, K. Kunimori, M. Sera, and F. Iga, Magnetic Field Induced $4f$ Octupole in CeB_6 Probed by Resonant X-Ray Diffraction, Phys. Rev. Lett. **103**, 017203 (2009).
[15] H. Watanabe and Y. Yanase, Group-theoretical classification of multipole order: Emergent responses and candidate materials, Phys. Rev. B **98**, 245129 (2018).
[16] S. Hayami, M. Yatsushiro, Y. Yanagi, and H. Kusunose, Classification of atomic-scale multipoles under crystallographic point groups and application to linear response tensors, Phys. Rev. B **98**, 165110 (2018).
[17] Y. Gao, D. Vanderbilt, and D. Xiao, Microscopic theory of spin toroidization in periodic crystals, Phys. Rev. B **97**, 134423 (2018).
[18] Y. Gao and D. Xiao, Orbital magnetic quadrupole moment and nonlinear anomalous thermoelectric transport, Phys. Rev. B **98**, 060402 (2018).
[19] A. Shitade, H. Watanabe, and Y. Yanase, Theory of orbital magnetic quadrupole moment and magnetoelectric susceptibility, Phys. Rev. B **98**, 020407 (2018).
[20] A. Shitade, A. Daido, and Y. Yanase, Theory of spin magnetic quadrupole moment and temperature-gradient-induced magnetization, Phys. Rev. B **99**, 024404 (2019).
[21] V. Dubovik and V. Tugushev, Toroid moments in electrodynamics and solid-state physics, Physics Reports **187**, 145 (1990).
[22] A. A. Gorbatsevich and Y. V. Kopaev, Toroidal order in crystals, Ferroelectrics **161**, 321 (1994), https://doi.org/10.1080/00150199408213381.

[23] C. Ederer and N. A. Spaldin, Towards a microscopic theory of toroidal moments in bulk periodic crystals, Phys. Rev. B **76**, 214404 (2007).

[24] N. A. Spaldin, M. Fiebig, and M. Mostovoy, The toroidal moment in condensed-matter physics and its relation to the magnetoelectric effect, Journal of Physics: Condensed Matter **20**, 434203 (2008).

[25] T.-h. Arima, J.-H. Jung, M. Matsubara, M. Kubota, J.-P. He, Y. Kaneko, and Y. Tokura, Resonant Magnetoelectric X-ray Scattering in GaFeO3: Observation of Ordering of Toroidal Moments, Journal of the Physical Society of Japan **74**, 1419 (2005), https://doi.org/10.1143/JPSJ.74.1419.

[26] B. B. Van Aken, J.-P. Rivera, H. Schmid, and M. Fiebig, Observation of ferrotoroidic domains, Nature **449**, 702 (2007).

[27] S. Hayami, H. Kusunose, and Y. Motome, Toroidal order in metals without local inversion symmetry, Phys. Rev. B **90**, 024432 (2014).

[28] C. D. Batista, G. Ortiz, and A. A. Aligia, Ferrotoroidic Moment as a Quantum Geometric Phase, Phys. Rev. Lett. **101**, 077203 (2008).

[29] F. Thöle, M. Fechner, and N. A. Spaldin, First-principles calculation of the bulk magnetoelectric monopole density: Berry phase and Wannier function approaches, Phys. Rev. B **93**, 195167 (2016).

[30] H. Watanabe and Y. Yanase, Magnetic hexadecapole order and magnetopiezoelectric metal state in $\mathbf{Ba}_{1-x}\mathbf{K}_x\mathbf{Mn}_2\mathbf{As}_2$, Phys. Rev. B **96**, 064432 (2017).

[31] M.-T. Suzuki, T. Koretsune, M. Ochi, and R. Arita, Cluster multipole theory for anomalous Hall effect in antiferromagnets, Phys. Rev. B **95**, 094406 (2017).

[32] I. V. Solovyev, Magneto-optical effect in the weak ferromagnets $LaMO_3$ (M= Cr, Mn, and Fe), Phys. Rev. B **55**, 8060 (1997).

[33] T. Tomizawa and H. Kontani, Anomalous Hall effect in the t_{2g} orbital kagome lattice due to noncollinearity: Significance of the orbital Aharonov-Bohm effect, Phys. Rev. B **80**, 100401 (2009).

[34] K. Ohgushi, S. Murakami, and N. Nagaosa, Spin anisotropy and quantum Hall effect in the kagomé lattice: Chiral spin state based on a ferromagnet, Phys. Rev. B **62**, R6065 (2000).

[35] R. Shindou and N. Nagaosa, Orbital Ferromagnetism and Anomalous Hall Effect in Antiferromagnets on the Distorted fcc Lattice, Phys. Rev. Lett. **87**, 116801 (2001).

[36] H. Chen, Q. Niu, and A. H. MacDonald, Anomalous Hall Effect Arising from Noncollinear Antiferromagnetism, Phys. Rev. Lett. **112**, 017205 (2014).

[37] J. Kübler and C. Felser, Non-collinear antiferromagnets and the anomalous Hall effect, EPL (Europhysics Letters) **108**, 67001 (2014).

[38] S. Nakatsuji, N. Kiyohara, and T. Higo, Large anomalous Hall effect in a non-collinear antiferromagnet at room temperature, Nature **527**, 212 (2015).

[39] A. K. Nayak, J. E. Fischer, Y. Sun, B. Yan, J. Karel, A. C. Komarek, C. Shekhar, N. Kumar, W. Schnelle, J. Kübler, C. Felser, and S. S. P. Parkin, Large anomalous Hall effect driven by a nonvanishing Berry curvature in the noncolinear antiferromagnet Mn_3Ge, Science Advances **2**, e1501870 (2016).

[40] X. Zhou, J.-P. Hanke, W. Feng, F. Li, G.-Y. Guo, Y. Yao, S. Blügel, and Y. Mokrousov, Spin-order dependent anomalous Hall effect and magneto-optical effect in the noncollinear antiferromagnets Mn_3XN with X = Ga, Zn, Ag, or Ni, Phys. Rev. B **99**, 104428 (2019).

[41] G. Gurung, D.-F. Shao, T. R. Paudel, and E. Y. Tsymbal, Anomalous Hall conductivity of noncollinear magnetic antiperovskites, Phys. Rev. Materials **3**, 044409 (2019).

[42] D. Boldrin, I. Samathrakis, J. Zemen, A. Mihai, B. Zou, F. Johnson, B. D. Esser, D. W. McComb, P. K. Petrov, H. Zhang, and L. F. Cohen, Anomalous Hall effect in noncollinear antiferromagnetic Mn_3NiN thin films, Phys. Rev. Materials **3**, 094409 (2019).

[43] K. Zhao, T. Hajiri, H. Chen, R. Miki, H. Asano, and P. Gegenwart, Anomalous Hall effect in the noncollinear antiferromagnetic antiperovskite $Mn_3Ni_{1-x}Cu_xN$, Phys. Rev. B **100**, 045109 (2019).

[44] Z. Q. Liu, H. Chen, J. M. Wang, J. H. Liu, K. Wang, Z. X. Feng, H. Yan, X. R. Wang, C. B. Jiang, J. M. D. Coey, and A. H. MacDonald, Electrical switching of the topological anomalous Hall effect in a non-collinear antiferromagnet above room temperature, Nature Electronics **1**, 172 (2018).

[45] L. Šmejkal, R. González-Hernández, T. Jungwirth, and J. Sinova, Crystal time-reversal symmetry breaking and spontaneous Hall effect in collinear antiferromagnets, Science Advances **6**, eaaz8809 (2020).

[46] H. Chen, T.-C. Wang, D. Xiao, G.-Y. Guo, Q. Niu, and A. H. MacDonald, Manipulating anomalous Hall antiferromagnets with magnetic fields, Phys. Rev. B **101**, 104418 (2020).

[47] H. Chen, Electronic chiralization as an indicator of the anomalous Hall effect in unconventional magnetic systems, Phys. Rev. B **106**, 024421 (2022).

[48] L. Rondin, J.-P. Tetienne, T. Hingant, J.-F. Roch, P. Maletinsky, and V. Jacques, Magnetometry with nitrogen-vacancy defects in diamond, Reports on Progress in Physics **77**, 056503 (2014).

[49] G. Q. Yan, S. Li, H. Lu, M. Huang, Y. Xiao, L. Wernert, J. A. Brock, E. E. Fullerton, H. Chen, H. Wang, and C. R. Du, Quantum Sensing and Imaging of Spin–Orbit-Torque-Driven Spin Dynamics in the Non-Collinear Antiferromagnet Mn3Sn, Advanced Materials **34**, 2200327 (2022), https://onlinelibrary.wiley.com/doi/pdf/10.1002/adma.202200327.

[50] S. Li, M. Huang, H. Lu, N. J. McLaughlin, Y. Xiao, J. Zhou, E. E. Fullerton, H. Chen, H. Wang, and C. R. Du, Nanoscale Magnetic Domains in Polycrystalline Mn3Sn Films Imaged by a Scanning Single-Spin Magnetometer, Nano Letters **23**, 5326 (2023).

[51] Y. Tokura and N. Nagaosa, Nonreciprocal responses from non-centrosymmetric quantum materials, Nature Communications **9**, 3740 (2018).

[52] S. A. Wolf, D. D. Awschalom, R. A. Buhrman, J. M. Daughton, S. von Molnár, M. L. Roukes, A. Y. Chtchelkanova, and D. M. Treger, Spintronics: A Spin-Based Electronics Vision for the Future, Science **294**, 1488 (2001), https://www.science.org/doi/pdf/10.1126/science.1065389.

[53] D. Ralph and M. Stiles, Spin transfer torques, Journal of Magnetism and Magnetic Materials **320**, 1190 (2008).

[54] S. Bader and S. Parkin, Spintronics, Annual Review of Condensed Matter Physics **1**, 71 (2010), https://doi.org/10.1146/annurev-conmatphys-070909-104123.

[55] L. Berger, Emission of spin waves by a magnetic multilayer traversed by a current, Phys. Rev. B **54**, 9353 (1996).

[56] J. Slonczewski, Current-driven excitation of magnetic multilayers, Journal of Magnetism and Magnetic Materials **159**, L1 (1996).

[57] A. Brataas, A. D. Kent, and H. Ohno, Current-induced torques in magnetic materials, Nature Materials **11**, 372 (2012).

[58] A. Manchon, J. Železný, I. M. Miron, T. Jungwirth, J. Sinova, A. Thiaville, K. Garello, and P. Gambardella, Current-induced spin-orbit torques in ferromagnetic and antiferromagnetic systems, Rev. Mod. Phys. **91**, 035004 (2019).

[59] Q. Shao, P. Li, L. Liu, H. Yang, S. Fukami, A. Razavi, H. Wu, K. Wang, F. Freimuth, Y. Mokrousov, M. D. Stiles, S. Emori, A. Hoffmann, J. Åkerman, K. Roy, J.-P. Wang, S.-H. Yang, K. Garello, and W. Zhang, Roadmap of Spin–Orbit Torques, IEEE Transactions on Magnetics **57**, 1 (2021).

[60] M. Kimata, H. Chen, K. Kondou, S. Sugimoto, P. K. Muduli, M. Ikhlas, Y. Omori, T. Tomita, A. H. MacDonald, S. Nakatsuji, and Y. Otani, Magnetic and magnetic-inverse spin Hall effects in a non-collinear antiferromagnet, Nature **565**, 627 (2019).

[61] K. Kondou, H. Chen, T. Tomita, M. Ikhlas, T. Higo, A. H. MacDonald, S. Nakatsuji, and Y. Otani, Giant field-like torque by the out-of-plane magnetic spin Hall effect in a topological antiferromagnet, Nature Communications **12**, 6491 (2021).

[62] J. Shi, P. Zhang, D. Xiao, and Q. Niu, Proper Definition of Spin Current in Spin-Orbit Coupled Systems, Phys. Rev. Lett. **96**, 076604 (2006).

[63] C. Xiao and Q. Niu, Conserved current of nonconserved quantities, Phys. Rev. B **104**, L241411 (2021).

[64] R. Resta, Macroscopic polarization in crystalline dielectrics: the geometric phase approach, Rev. Mod. Phys. **66**, 899 (1994).

[65] R. D. King-Smith and D. Vanderbilt, Theory of polarization of crystalline solids, Phys. Rev. B **47**, 1651 (1993).

[66] D. Xiao, J. Shi, and Q. Niu, Berry Phase Correction to Electron Density of States in Solids, Phys. Rev. Lett. **95**, 137204 (2005).

[67] T. Thonhauser, D. Ceresoli, D. Vanderbilt, and R. Resta, Orbital Magnetization in Periodic Insulators, Phys. Rev. Lett. **95**, 137205 (2005).

[68] J. Shi, G. Vignale, D. Xiao, and Q. Niu, Quantum Theory of Orbital Magnetization and Its Generalization to Interacting Systems, Phys. Rev. Lett. **99**, 197202 (2007).

[69] M. F. Lapa and T. L. Hughes, Semiclassical wave packet dynamics in nonuniform electric fields, Phys. Rev. B **99**, 121111 (2019).

[70] A. Daido, A. Shitade, and Y. Yanase, Thermodynamic approach to electric quadrupole moments, Phys. Rev. B **102**, 235149 (2020).

[71] H. Chen, G.-Y. Guo, D. Xiao, *et al.*, in preparation.

[72] I. Garate and A. H. MacDonald, Influence of a transport current on magnetic anisotropy in gyrotropic ferromagnets, Phys. Rev. B **80**, 134403 (2009).

[73] F. Freimuth, S. Blügel, and Y. Mokrousov, Spin-orbit torques in Co/Pt(111) and Mn/W(001) magnetic bilayers from first principles, Phys. Rev. B **90**, 174423 (2014).

[74] K. M. D. Hals and A. Brataas, Spin-motive forces and current-induced torques in ferromagnets, Phys. Rev. B **91**, 214401 (2015).

[75] F. Freimuth, S. Blügel, and Y. Mokrousov, Direct and inverse spin-orbit torques, Phys. Rev. B **92**, 064415 (2015).

[76] S. A. Vitale, D. Nezich, J. O. Varghese, P. Kim, N. Gedik, P. Jarillo-Herrero, D. Xiao, and M. Rothschild, Valleytronics: Opportunities, Challenges, and Paths Forward, Small **14**, 1801483 (2018), https://onlinelibrary.wiley.com/doi/pdf/10.1002/smll.201801483.

[77] W. Yao, D. Xiao, and Q. Niu, Valley-dependent optoelectronics from inversion symmetry breaking, Phys. Rev. B **77**, 235406 (2008).

[78] H. Zeng, J. Dai, W. Yao, D. Xiao, and X. Cui, Valley polarization in MoS2 monolayers by optical pumping, Nature Nanotechnology **7**, 490 (2012).

[79] E. J. Sie, J. W. McIver, Y.-H. Lee, L. Fu, J. Kong, and N. Gedik, Valley-selective optical Stark effect in monolayer WS2, Nature Materials **14**, 290 (2015).

[80] K. Huang, On the Zitterbewegung of the Dirac Electron, American Journal of Physics **20**, 479 (1952), https://doi.org/10.1119/1.1933296.

[81] M.-C. Chang and Q. Niu, Berry curvature, orbital moment, and effective quantum theory of electrons in electromagnetic fields, Journal of Physics: Condensed Matter **20**, 193202 (2008).

[82] D. Culcer, Y. Yao, and Q. Niu, Coherent wave-packet evolution in coupled bands, Phys. Rev. B **72**, 085110 (2005).

[83] D. Culcer and Q. Niu, Geometrical phase effects on the Wigner distribution of Bloch electrons, Phys. Rev. B **74**, 035209 (2006).

[84] J. D. Jackson, *Classical electrodynamics; 3rd ed.* (Wiley, New York, NY, 1999).

[85] See Supplementary Material at [url] for technical details, which includes Refs. [86-96].

[86] N. Marzari, A. A. Mostofi, J. R. Yates, I. Souza, and D. Vanderbilt, Maximally localized Wannier functions: Theory and applications, Rev. Mod. Phys. **84**, 1419 (2012).

[87] D. Xiao, M.-C. Chang, and Q. Niu, Berry phase effects on electronic properties, Rev. Mod. Phys. **82**, 1959 (2010).

[88] E. Blount, Formalisms of Band Theory (Academic Press, 1962) pp. 305–373.

[89] L. L. Hirst, The microscopic magnetization: concept and application, Rev. Mod. Phys. **69**, 607 (1997).

[90] A. N. Rudenko, S. Yuan, and M. I. Katsnelson, Toward a realistic description of multilayer black phosphorus: From *GW* approximation to large-scale tight-binding simulations, Phys. Rev. B **92**, 085419 (2015).

[91] D. J. P. de Sousa, L. V. de Castro, D. R. da Costa, J. M. Pereira, and T. Low, Multilayered black phosphorus: From a tight-binding to a continuum description, Phys. Rev. B **96**, 155427 (2017).

[92] S. Fukuoka, T. Taen, and T. Osada, Electronic Structure and the Properties of Phosphorene and Few-Layer Black Phosphorus, Journal of the Physical Society of Japan **84**, 121004 (2015), https://doi.org/10.7566/JPSJ.84.121004.

[93] S. S. Baik, K. S. Kim, Y. Yi, and H. J. Choi, Emergence of Two-Dimensional Massless Dirac Fermions, Chiral Pseudospins, and Berry's Phase

in Potassium Doped Few-Layer Black Phosphorus, Nano Letters **15**, 7788 (2015), pMID: 26572058, https://doi.org/10.1021/acs.nanolett.5b04106.

[94] Z. S. Popović, J. M. Kurdestany, and S. Satpathy, Electronic structure and anisotropic Rashba spin-orbit coupling in monolayer black phosphorus, Phys. Rev. B **92**, 035135 (2015).

[95] Y. Yao, L. Kleinman, A. H. MacDonald, J. Sinova, T. Jungwirth, D.-s. Wang, E. Wang, and Q. Niu, First Principles Calculation of Anomalous Hall Conductivity in Ferromagnetic bcc Fe, Phys. Rev. Lett. **92**, 037204 (2004).

[96] X. Wang, J. R. Yates, I. Souza, and D. Vanderbilt, Ab initio calculation of the anomalous Hall conductivity by Wannier interpolation, Phys. Rev. B **74**, 195118 (2006).

[97] I. Sodemann and L. Fu, Quantum Nonlinear Hall Effect Induced by Berry Curvature Dipole in Time-Reversal Invariant Materials, Phys. Rev. Lett. **115**, 216806 (2015).

[98] C. Xiao, H. Chen, Y. Gao, D. Xiao, A. H. MacDonald, and Q. Niu, Linear magnetoresistance induced by intra-scattering semiclassics of Bloch electrons, Phys. Rev. B **101**, 201410 (2020).

[99] D. Culcer, J. Sinova, N. A. Sinitsyn, T. Jungwirth, A. H. MacDonald, and Q. Niu, Semiclassical Spin Transport in Spin-Orbit-Coupled Bands, Phys. Rev. Lett. **93**, 046602 (2004).

[100] K. Nomura, J. Wunderlich, J. Sinova, B. Kaestner, A. H. MacDonald, and T. Jungwirth, Edge-spin accumulation in semiconductor two-dimensional hole gases, Phys. Rev. B **72**, 245330 (2005).

[101] W.-K. Tse, J. Fabian, I. Žutić, and S. Das Sarma, Spin accumulation in the extrinsic spin Hall effect, Phys. Rev. B **72**, 241303 (2005).

[102] S. Murakami, Quantum Spin Hall Effect and Enhanced Magnetic Response by Spin-Orbit Coupling, Phys. Rev. Lett. **97**, 236805 (2006).

[103] A. N. Rudenko and M. I. Katsnelson, Quasiparticle band structure and tight-binding model for single- and bilayer black phosphorus, Phys. Rev. B **89**, 201408 (2014).

[104] M. Ezawa, Topological origin of quasi-flat edge band in phosphorene, New Journal of Physics **16**, 115004 (2014).

[105] A. Chaves, W. Ji, J. Maassen, T. Dumitrică, and T. Low, Theoretical Overview of Black Phosphorus, in *2D Materials: Properties and Devices*, edited by P. Avouris, T. F. Heinz, and T. Low (Cambridge University Press, 2017) p. 381–412.

[106] S. M. Farzaneh and S. Rakheja, Extrinsic spin-orbit coupling and spin relaxation in phosphorene, Phys. Rev. B **100**, 245429 (2019).

[107] H. Chen, Q. Niu, and A. H. MacDonald, Spin Hall effects without spin currents in magnetic insulators (2019), arXiv:1803.01294 [cond-mat.mes-hall].

[108] V. Kozii, A. Avdoshkin, S. Zhong, and J. E. Moore, Intrinsic Anomalous Hall Conductivity in a Nonuniform Electric Field, Phys. Rev. Lett. **126**, 156602 (2021).

[109] L. Dong, *Geometrodynamics in crystals with space-time periodicity and deformation*, Ph.D. thesis, The University of Texas at Austin (2021).